Reprint Series
12 April 1996, Volume 272, pp. 234–238

SCIENCE

Global Observations of Oceanic Rossby Waves

Dudley B. Chelton* and Michael G. Schlax

Global Observations of Oceanic Rossby Waves

Dudley B. Chelton* and Michael G. Schlax

Rossby waves play a critical role in the transient adjustment of ocean circulation to changes in large-scale atmospheric forcing. The TOPEX/POSEIDON satellite altimeter has detected Rossby waves throughout much of the world ocean from sea level signals with $\lesssim$10-centimeter amplitude and $\gtrsim$500-kilometer wavelength. Outside of the tropics, Rossby waves are abruptly amplified by major topographic features. Analysis of 3 years of data reveals discrepancies between observed and theoretical Rossby wave phase speeds that indicate that the standard theory for free, linear Rossby waves is an incomplete description of the observed waves.

One of the major breakthroughs in the development of a theoretical understanding of the large-scale circulations of the ocean and atmosphere was Carl Gustave Rossby's discovery in the 1930s (*1*) of a special class of waves that owe their existence to the spherical shape of the Earth. These planetary Rossby waves (*2*) are easily observed in the atmosphere as the large meanders of the mid-latitude jet stream that are responsible for the prevailing seasonal weather patterns and their day-to-day variations. Rossby waves have been much more difficult to detect in the ocean because of their small sea-surface signature (height variations of order 10 cm or smaller), slow propagation speeds (of order 10 cm s^{-1} or less), and long wavelengths (hundreds to thousands of kilometers). We present here a summary of global observations of oceanic Rossby waves from the joint United States–French TOPEX/POSEIDON satellite altimeter mission and a comparison of the observations with predictions based on the standard theory for freely propagating, linear Rossby waves.

Rossby waves are central to all modern theories of large-scale ocean circulation. They are responsible for establishing the most fundamental feature of the large-scale circulation: the westward intensification of circulation gyres (*3*). In the North Atlantic, this is manifest as the intense Gulf Stream western boundary current. There are counterparts in the other major ocean basins. Rossby waves are also the dynamical mechanism for the transient adjustment of the ocean to changes in large-scale atmospheric forcing. In concert with coastal-trapped waves along the eastern boundary of an ocean basin, Rossby waves are a mechanism for transmitting information from the tropical ocean to the middle and high-latitude interior ocean (*4*). It has recently been suggested (*5*) that Rossby waves generated by El Niño events (*6*) may account for ocean circulation anomalies a decade later in the mid-latitude North Pacific. Such ocean changes might significantly influence weather patterns over North America.

Theoretical background. Rossby waves are the large-scale dynamical response of the ocean to wind forcing and buoyancy forcing (heating and cooling) at the eastern boundaries and over the ocean interior. They can also be generated by perturbations along the eastern boundaries associated with coastal-trapped waves originating at lower latitudes. Although it is possible for Rossby wave characteristics (amplitude and propagation speed) to be altered by wind or buoyancy forcing that is coherent with the wave at precise wave numbers and frequencies (*7*), there is no evidence at present to indicate that such resonance exists over the broad ranges of wave numbers and frequencies and the global geographical domain over which sea level signals with Rossby wave–like characteristics are observed in

The authors are at the College of Oceanic and Atmospheric Sciences, Oregon State University, Corvallis, OR 97331–5503, USA.

*To whom correspondence should be addressed.

the TOPEX/POSEIDON data analyzed here. The premise of this analysis is that Rossby waves generated by forcing at the eastern boundary or over the ocean interior subsequently propagate away from the source as free waves.

The standard theory for freely propagating, linear Rossby waves can be derived from a linearization of the unforced equations for large-scale, low-frequency motion about a state of rest. This yields a wave equation for the vertical normal modes (*8*). The restoring force is the so-called "β effect" of latitudinal variation of the local vertical component of the Earth's angular rotation vector. The curvature of the Earth's surface is thus essential to the existence of Rossby waves.

With appropriate surface and bottom boundary conditions, one can determine the normal modes numerically by solving an eigenvalue problem that depends only on the local stratification (*8–10*). There exist an infinite number of Rossby wave normal modes, ordered by decreasing phase speed. The phase speeds are westward for all of the modes, and low-frequency, long-wavelength solutions are zonally nondispersive (that is, the westward component of phase speed is independent of wavelength).

The lowest order (barotropic) mode is uniform vertically, independent of stratification, and propagates across an entire ocean basin in a period of about a week. This is too fast to be resolved in measurements from an orbiting satellite. The next higher order (first baroclinic) mode is surface intensified, depends strongly on the stratification, has a velocity profile that changes sign at the depth of the thermocline (*11*), and propagates much more slowly, requiring months to decades to cross an ocean basin (Fig. 1). The basin crossing time increases with increasing latitude because of the latitudinal variation of phase speed owing to the β effect. As a result, the crests and troughs of Rossby waves initiated simultaneously along the entire eastern boundary of an ocean basin arrive at the western boundary much sooner at low latitudes than at high latitudes, an effect often referred to as β refraction.

An important feature of the first baroclinic mode is that variations of the sea surface height are mirrored as thermocline depth variations of the opposite sign with about three orders of magnitude greater amplitude (*8*). A sea level variation of 5 cm thus corresponds to a thermocline displacement of about 50 m. Such large variations of upper ocean thermal structure have important implications about the role of the ocean in short-term climate variations.

In most regions of the ocean, it is generally believed that the slower, higher order baroclinic Rossby wave modes play a lesser role in large-scale ocean circulation dynamics. The focus here is therefore on first-mode baroclinic Rossby waves.

Observations of westward propagation. Evidence of first-mode baroclinic Rossby waves has been presented from ship-based measurements of the upper ocean thermal structure (*7, 12*). Because most of the ocean is severely undersampled, unambiguous interpretation of Rossby wave signals in the thermal measurements is difficult at all but a small number of locations.

The advent of satellite altimetry in the late 1970s established a foundation for global observations of baroclinic Rossby waves (*13*). The measurement accuracy and mission duration of the early GEOS-3 and SEASAT altimeters (*14*) were inadequate for detecting Rossby waves. The GEOSAT altimeter (*15*) measured sea level from 1985 through 1989 with sufficient accuracy (*16, 17*), but the orbit configuration was ill suited to Rossby wave studies because tidal errors aliased into wave numbers and frequencies that are difficult to distinguish from annual-period baroclinic Rossby waves (*18, 19*).

The TOPEX/POSEIDON altimeter, launched in August 1992 into a 10-day, exactly repeating orbit cycle, is the first flown in an orbit specifically designed to avoid tidal aliasing (*19, 20*). An essentially continuous record of sea level measurements with an accuracy of ~4 cm has been obtained since the instruments became fully operational in October 1992 (*21*). Large-scale sea level signals with amplitudes as small as ~1 cm can be detected after appropriate filtering of the data to reduce the quasi-random component of measurement errors. The >3-year data record thus provides the ability to detect Rossby waves unambiguously over the entire world ocean.

For the analysis presented here, the TOPEX/POSEIDON data were filtered (*22*) specifically to highlight the long Rossby waves predicted by the theoretical considerations outlined above. The expected westward propagation of alternating positive and negative sea level signals is a very common feature in the resulting filtered sea level fields (Figs. 2 and 3). The periods of these signals generally fall between 0.5 and 2 cycles per year, and the wavelengths typically range from 10,000 km or longer in the tropics to about 500 km at 50° latitude. These propagating signals account for more than 30% of the total sea level variance at latitudes lower than 15° but only about 10% of the variance at latitudes higher than 30°. The mechanisms that generate this widespread propagation have not yet been determined. In many cases, the waves originate at the eastern boundaries of ocean basins, either from local wind or buoyancy forcing or in association with coastal-trapped waves originating at lower latitudes. In some cases, the waves appear to originate in the ocean interior.

The propagating signals in the extratropical examples (Fig. 2) are larger in amplitude west of major topographic features (the Emperor Seamounts at 170°E, 39°N; the southeast flank of Hess Rise at 175°W, 32°N; and the Hawaiian Ridge at 155°W, 21°N). This relation between bottom topography and wave amplitude has previously been reported in the North Atlantic (*17, 19*). It is observed in this analysis in many

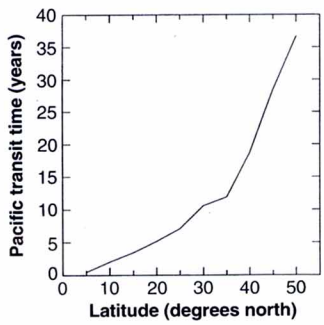

Fig. 1. Latitudinal variation of the time required for baroclinic Rossby waves to cross an ocean basin with the geometry of the North Pacific. These transit times are based on the phase speeds predicted by the standard theory for freely propagating, nondispersive, linear, first-mode baroclinic Rossby waves (*10*).

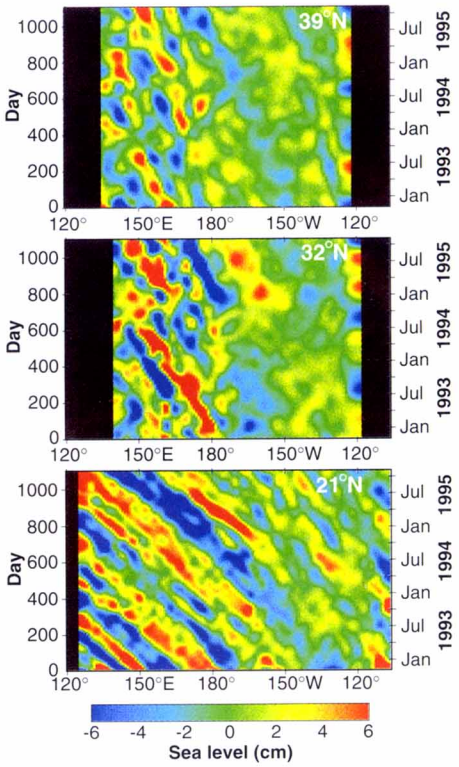

Fig. 2. Time-longitude sections of filtered sea level (*22*) in the Pacific Ocean along 39°, 32°, and 21°N. These examples are representative of extratropical latitudes throughout the world ocean.

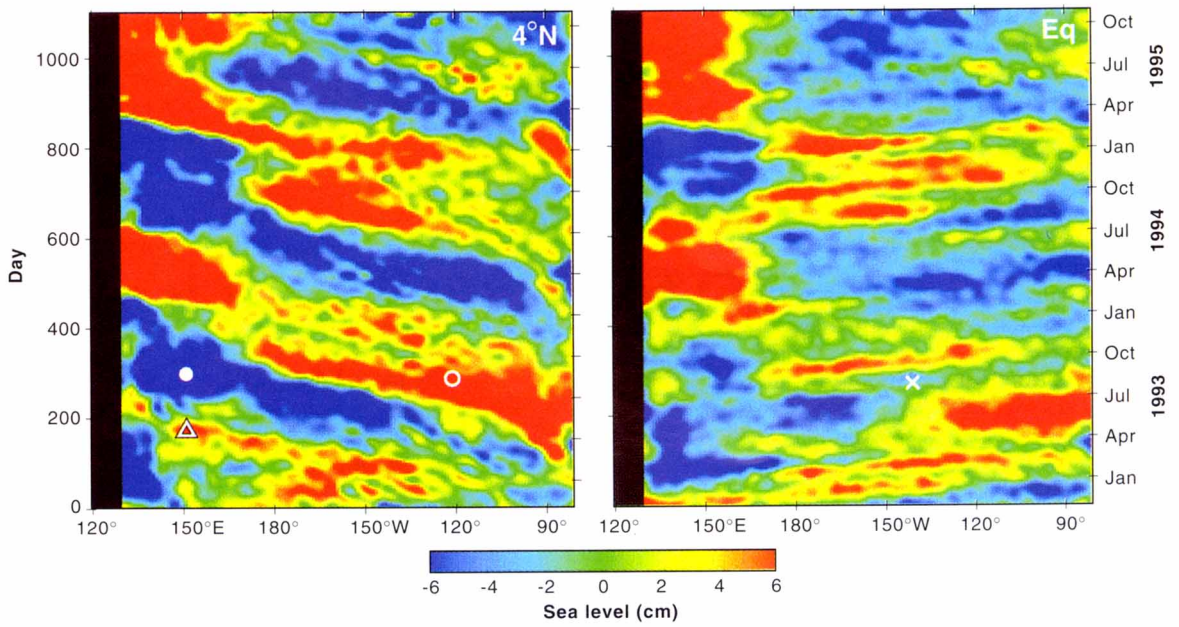

Fig. 3. Time-longitude sections of filtered sea level (*22*) in the Pacific Ocean along 4°N and the equator. A section along 4°S is almost identical to the 4°N section. The time axis is stretched compared with Fig. 2 to aid in the identification of the rapid eastward- and westward-propagating tropical sea level signals. The symbols correspond to the times and locations of the matching symbols in Fig. 4.

of the time-longitude sections of TOPEX/POSEIDON data throughout the world ocean. In the 21°N and 39°N examples, the westward-propagating signals appear to originate at the eastern boundary and abruptly amplify over the mid-ocean topography. In the 32°N example, there is no detectable westward propagation east of Hess Rise, suggesting that the topography may be a source of the waves.

Previous theoretical studies have suggested at least three possible ways that topography could affect baroclinic Rossby waves (*23*). Additional analysis is required to identify the mechanism responsible for the strong topographic interaction observed by TOPEX/POSEIDON. Also in need of further study is the surprisingly weak westward penetration of the observed energetic sea level variability near the eastern boundary (Fig. 2), presumably associated with seasonal wind forcing.

Another common feature in the data is an increase of the phase speed of the observed waves in the western basins. This phenomenon is evident in the 21°N example, where the phase speed in the far western basin exceeds that in the far eastern basin by more than 50%. This longitudinal variation of phase speed is a consequence of the deepening of the thermocline in the west (*10*).

Waves within about 2° of the equator are distinctly different from extratropical waves. Most of the observed sea level variability along the equator consists of eastward-propagating signals with phase speeds of about 270 cm s^{-1} (Fig. 3). These signals can be interpreted as equatorially trapped Kelvin waves, often originating in the central Pacific where they are generated by short-period equatorial wind events at about 170°E (*24*–*26*). It has recently been suggested (*24*) that these intraseasonal Kelvin waves may play an important role in the onset of interannual El Niño events.

Superimposed on the rapidly propagating, short-period Kelvin waves are two long-period, relatively slow, eastward-propagating, positive sea level signals. The first originated at the western boundary in October 1992 and reached the eastern boundary in June 1993, and the second originated in June 1994 and reached the eastern boundary in January 1995. These signals are

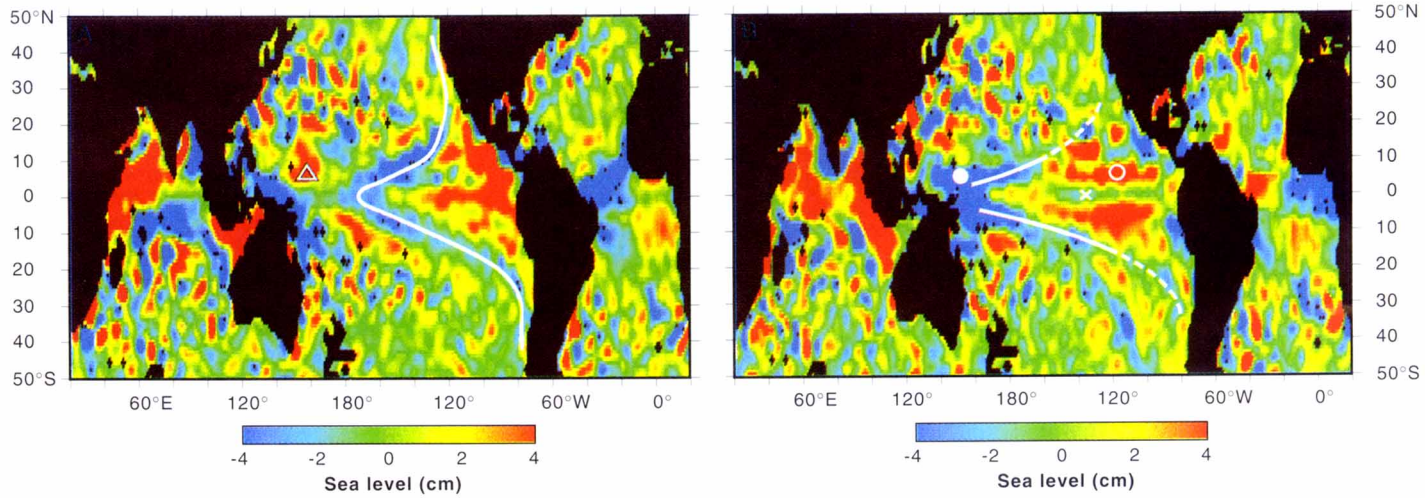

Fig. 4. Global maps of filtered sea level (*22*) on (**A**) 13 April 1993 (cycle 21) and 3.5 months later on (**B**) 31 July 1993 (cycle 32). White lines identify a westward-propagating, β-refracted Rossby wave trough. The time evolutions of the equatorial Kelvin wave trough (X), the Rossby wave crests (open triangle and open circle), and the Rossby wave trough (solid circle) can be traced from the times and locations of the matching symbols in Fig. 3. These two maps are frames from an animation of TOPEX/POSEIDON data that is available on the World Wide Web at http://topex-www.jpl.nasa.gov/contrib/chelton/rossby/.

coincident with the second and third pulses of the recent, long-lasting El Niño event (*27*). Because their propagation speed is only about one-third that of Kelvin waves, these slow eastward-propagating signals are likely coupled atmosphere-ocean phenomena (*6*) rather than freely propagating waves.

In addition to the fast and slow eastward-propagating equatorial signals, there are smaller amplitude, long-period westward-propagating sea level signals that can be interpreted as tropical Rossby waves with westward phase speeds of about 100 cm s^{-1} (*12, 24–26*). The latitudinal structure of sea level associated with the dominant tropical Rossby waves has a local minimum at the equator with symmetric maxima at about 4°N and 4°S (*25, 26*). The observed westward propagation is therefore much more apparent along 4°N than along the equator (Fig. 3). A noteworthy feature of these tropical Rossby waves is a monotonically increasing westward phase speed between the South American coast and about 140°W and relatively constant phase speed farther west. As with the geographical variation of the phase speeds of waves noted along 21°N, this shift is a consequence of the deepening of the thermocline in the western tropical Pacific (*10*).

Spatial structure of the observed Rossby waves. Two frames from an animation of the filtered TOPEX/POSEIDON data are shown in Fig. 4. In the 13 April 1993 frame, a negative sea level signal has propagated along the equator from South America to the far western Pacific. An elongated negative sea level pattern trailing behind the equatorial signal at higher latitudes can be traced to about 40° latitude in both hemispheres. This feature is characteristic of a β-refracted Rossby wave trough. The remnants of an earlier refracted Rossby wave crest are evident westward and poleward of the trough, and a new crest is seen to be forming in the far eastern tropical Pacific. Similar refracted Rossby wave crests and troughs can be seen in both the Atlantic and Indian oceans.

In the 31 July 1993 frame, the Rossby wave trough has impinged on the western boundary of the Pacific, and an equatorial Kelvin wave trough centered at about 140°W has propagated rapidly eastward more than halfway across the Pacific, splitting the newly formed Rossby wave crest that has propagated westward from South America. An important and controversial question presently under investigation (*26*) is whether equatorially trapped Kelvin waves such as this can be generated by the reflection of Rossby waves from the western boundary (a purely oceanic process) or whether the Kelvin waves are forced by trade wind variations in response to the changes of sea surface temperature associated with the Rossby waves (an air-sea interaction process). The dense coverage and continuing data record provided by TOPEX/POSEIDON are likely to provide important insight into this dynamical process.

Outside of the tropics, the positive and negative sea level signals lose their latitudinally coherent refractive structure soon after generation. The resulting discontinuous sea level features fluctuate in amplitude but continue propagating westward across the basin. The amplitude fluctuations are evident in the time-longitude sections in Fig. 2 as ripples along the propagating positive and negative sea level signals. The breakup of the coherent structures may be indicative of the effects of distortions of freely propagating waves by local wind forcing or bottom topography.

Comparison between observations and theory. Time-longitude sections like those in Figs. 2 and 3 were constructed throughout the world ocean. The phase speeds of westward-propagating signals estimated from these sections (*28*) are shown in Fig. 5. Although the strong latitudinal variation of these observed phase speeds is consistent with the expected β refraction of Rossby waves, the observed phase speeds outside of the tropical band from 10°N to 10°S are systematically greater than those predicted by the standard theory for freely propagating linear, first-mode baroclinic Rossby waves (*29*).

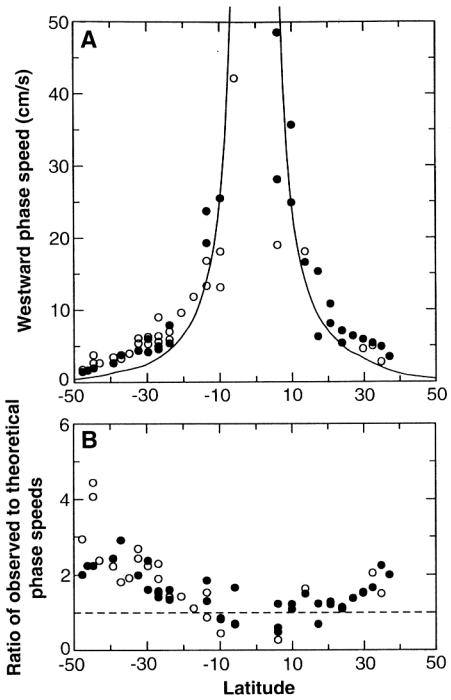

Fig. 5. (**A**) Globally distributed estimates of the phase speeds of westward-propagating sea level signals estimated from 3 years of TOPEX/POSEIDON altimeter observations. The solid circles correspond to Pacific estimates, and the open circles correspond to Atlantic and Indian Ocean estimates. The global average latitudinal variation of the phase speed predicted by the standard theory for extratropical freely propagating, nondispersive, linear, first-mode baroclinic Rossby waves (*10*) is superimposed as the continuous line. (**B**) Ratio of the observed phase speeds to the phase speeds predicted by the standard theory at the same geographical locations as the observations.

The discrepancies between observed and predicted phase speeds are too large to be artifacts. The possibility that they may have been spuriously introduced by sampling errors or data processing has also been ruled out on the basis of simulations of each of the processing steps applied to the TOPEX/POSEIDON data. We thus conclude that the standard theory for freely propagating, linear, baroclinic Rossby waves is deficient in predicting the observed phase speeds.

The inadequacy of the standard theory for prediction of Rossby wave phase speeds has been noted previously from upper ocean thermal data (*7, 12, 30*). Because of the paucity of in situ thermal measurements available for Rossby wave detection, these studies have been restricted to the region between 8° and 22°N in the Pacific. In addition to corroborating these widely unappreciated results, this analysis of TOPEX/POSEIDON data underscores the global significance of the deficiency of the standard theory for free, linear Rossby waves. At least two mechanisms have been suggested to explain the high observed phase speeds (*7, 31*), but the issue is not yet resolved.

The implication of these results is that the ocean reacts more rapidly than is generally believed; the transient baroclinic adjustment time of the ocean at 35° latitude, for example, is only about half as long as that predicted by the standard theory. The transoceanic transit times shown in Fig. 1 for the North Pacific must be modified to account for the observed propagation speeds of extratropical baroclinic Rossby waves. The TOPEX/POSEIDON observations of high phase speeds, as well as the apparent effects of bottom topography on extratropical Rossby waves (Fig. 2), provide important consistency checks for evaluating the performance of ocean general circulation models (*32*) for studies of the role of the ocean in interannual and decadal climate variability.

REFERENCES AND NOTES

1. C. G. Rossby *et al.*, *J. Mar. Res.* **2**, 38 (1939); C. G. Rossby, *Q. J. R. Meteorol. Soc.* **66**, 66 (1940).
2. G. W. Platzman, *Q. J. R. Meteorol. Soc.* **94**, 225 (1968).
3. D. L. T. Anderson and A. E. Gill, *Deep-Sea Res.* **22**, 583 (1975); D. L. T. Anderson, K. Bryan, A. E. Gill, R. C. Pacanowski, *J. Geophys. Res.* **84**, 4795 (1979).
4. J. P. McCreary, *J. Phys. Oceanogr.* **6**, 632 (1976); H. E. Hurlburt, J. C. Kindle, J. J. O'Brien, *ibid.*, p. 621.
5. G. A. Jacobs *et al.*, *Nature* **370**, 360 (1994).
6. T. P. Barnett, L. Latif, E. Kirk, E. Roeckner, *J. Clim.* **4**, 487 (1991); J. D. Neelin, M. Latif, F.-F. Jin, *Annu. Rev. Fluid Mech.* **26**, 617 (1994); D. S. Battisti and E. S.

Sarachik, *Rev. Geophys.* **33** (suppl.), 1367 (1995).
7. W. B. White, *J. Phys. Oceanogr.* **7**, 50 (1977); *ibid.* **15**, 403 (1985); and references therein.
8. P. H. LeBlond and L. A. Mysak, *Waves in the Ocean* (Elsevier, New York, 1978); A. E. Gill, *Atmosphere-Ocean Dynamics* (Academic Press, Cambridge, UK, 1982).
9. W. J. Emery, W. G. Lee, L. Magaard, *J. Phys. Oceanogr.* **14**, 294 (1984); S. Houry, E. Dombrowsky, P. DeMey, J.-F. Minster, *ibid.* **17**, 1619 (1987).
10. D. B. Chelton, M. G. Schlax, R. A. deSzoeke, K. El Naggar, N. Siwertz, in preparation.
11. The thermocline is the region of strong vertical gradients of temperature and density that separates the cold, dense, and nearly homogeneous deep water from the warm and weakly stratified upper water column.
12. W. S. Kessler, *J. Geophys. Res.* **95**, 5183 (1990).
13. L.-L. Fu and R. E. Cheney, *Rev. Geophys.* **33** (suppl.), 213 (1995).
14. A performance comparison between the GEOS-3, SEASAT, and GEOSAT altimeters and prelaunch expectations of TOPEX/POSEIDON is summarized by L.-L. Fu, D. B. Chelton, and V. Zlotnicki [*Oceanography* **1**, 4 (1988)].
15. B. C. Douglas and R. E. Cheney, *J. Geophys. Res.* **95**, 2833 (1990).
16. Examples of apparent Rossby waves inferred from regional analyses of GEOSAT data include P. E. Matthews, M. A. Johnson, J. J. O'Brien, *ibid.* **97**, 17829 (1992); C. Périgaud and P. Delecluse, *ibid.*, p. 20169; M. L. Van Woert and J. M. Price, *ibid.* **98**, 14619 (1993); P.-Y. Le Traon and J.-F. Minster, *ibid.*, p. 12315; S. Aoki, S. Imawaki, K. Ichikiawa, *ibid.* **100**, 839 (1995).
17. R. T. Tokmakian and P. G. Challenor, *J. Geophys. Res.* **98**, 4761 (1993).
18. G. A. Jacobs, G. H. Born, M. E. Parke, P. C. Allen, *ibid.* **97**, 17813 (1992); M. G. Schlax and D. B. Chelton, *ibid.* **99**, 12603 (1994).
19. M. G. Schlax and D. B. Chelton, *ibid.*, p. 24761.
20. M. E. Parke, R. H. Stewart, D. L. Farless, D. E. Cartwright, *ibid.* **92**, 11693 (1987).
21. L.-L. Fu *et al.*, *ibid.* **99**, 24369 (1994).
22. We smoothed the raw TOPEX/POSEIDON sea level observations to retain scales longer than 40 days and larger than 6° of latitude by 6° of longitude. Outside of the equatorial band of 5°S to 5°N, the smoothed sea level fields were further low-pass filtered to remove eddy signals with periods shorter than 100 days; the shorter time scales were retained at lower latitudes to resolve the short-period signals known to exist in the equatorial band (Fig. 3). We then removed longitudinally coherent sea level signals associated with the steric effects of heating and cooling. This refinement was achieved by zonally high-pass filtering the smoothed sea level fields along latitude θ to retain only scales shorter than 4×10^4 km for $\theta < 5°$ and shorter than $2 \times 10^5\ \theta^{-1}$ km for $\theta > 5°$.
23. P. B. Rhines, *J. Fluid Mech.* **37**, 161 (1969); B. Barnier, *J. Phys. Oceanogr.* **18**, 417 (1988); R. Gerdes and C. Wübber, *ibid.* **21**, 1300 (1991).
24. W. S. Kessler, M. J. McPhaden, K. M. Weickmann, *J. Geophys. Res.* **100**, 10613 (1995); W. S. Kessler and M. J. McPhaden, *J. Clim.* **8**, 1757 (1995).
25. T. Delcroix, J. Picaut, G. Eldin, *J. Geophys. Res.* **96**, 3249 (1991); T. Delcroix, J.-P. Boulanger, F. Masia, C. Menkes, *ibid.* **99**, 25093 (1994).
26. J.-P. Boulanger and C. Menkes, *ibid.* **100**, 25041 (1995); J.-P. Boulanger and L.-L. Fu, in preparation.
27. K. E. Trenberth and T. J. Hoar, *Geophys. Res. Lett.* **23**, 57 (1996).
28. The time-longitude plots were examined visually to identify regions of unambiguous westward propagation. The phase speed was then estimated objectively for each section for which the visible propagation spanned at least 30° of longitude. The objective estimate was obtained from an empirical version of the Radon transform, commonly referred to as a "slant stack" in the seismological literature [A. K. Jain, *Fundamentals of Digital Image Processing* (Prentice Hall, Englewood Cliffs, NJ, 1989); J. F. Claerbout, *Imaging the Earth's Interior* (Blackwell, Oxford, UK, 1985)]. Sea level was summed along lines of constant phase speed in the time-longitude plane for a range of phase speeds. The line sums along 100 sample lines for each phase speed were then squared and summed. The phase speed corresponding to the maximum sum of squares constitutes the empirical estimate of phase speed. Each objective estimate was visually checked for consistency with the time-longitude section from which it was constructed.
29. The standard theory considered here breaks down within about 10° of the equator, where the vertical component of the Earth's angular rotation vector becomes vanishingly small. An amended theory has been developed for the equatorial band [S. G. Philander, *El Niño, La Niña, and the Southern Oscillation* (Academic Press, San Diego, 1990)], and the observed phase speeds between 10°S and 10°N are consistent with the equatorial theory (*25, 26*).
30. G. Meyers, *J. Phys. Oceanogr.* **9**, 664 (1979).
31. D. L. T. Anderson and P. D. Killworth, *Deep-Sea Res. A* **26**, 1033 (1979).
32. J. K. Dukowicz and R. D. Smith, *J. Geophys. Res.* **99**, 7991 (1994); A. J. Semtner, *Science* **269**, 1379 (1995).
33. This research was supported by contract 958127 from the Jet Propulsion Laboratory, by grant NAGW-3510 from the National Aeronautics and Space Administration, and by grant OCE-9402856 from NSF. We thank R. deSzoeke, M. Freilich, S. Imawaki, W. Kessler, R. Matano, R. Miller, R. Stewart, T. Strub, and D. Witter for comments.

21 November 1995; accepted 26 February 1996